

E. Furuta, N. Iwasaki, R. Okumura¹ and Y. Inuma¹

Ochanomizu University

¹*Research Reactor Institute, Kyoto University*

INTRODUCTION: Chinese medicines and herbs were analyzed in a previous experiment at KUR. At that results, toxic elements of As and Hg were contained with high concentrations in 2 Chinese medicine; *Niu Huang Jiedu Pian* and *Liushen Wan*. However, when they are sulphide, they were not absorbed into the body. So, the chemical structures are very important. Furthermore, low concentrations of Hg were contained in many Chinese medicines and herbs. However, Chinese medicines and herbs produced in Japan contained these toxic elements rarely. The previous experiment raised mainly 3 queries; 1. Do the same named medicines contain same toxic elements with same level concentrations? 2. What chemical structures were the As and Hg? 3. Do not Chinese medicines and herbs produced in Japan contain toxic elements? The purpose of this study was to clear these issues.

EXPERIMENTS: Additional samples used in this study were 30. (The total sample number was 149.) They were grinded into powders with an agate mortar and enclosed each in a double polyethylene bag by measuring their weight. The standard samples used were JA-2 and JR-2 of rock standard, and 50 ppm of As, Hg, Sb, Co and Cr of atomic absorption reagents (Wako) were used applying to 5 filter papers (Advantec 5A). The samples and the standards were irradiated $1\text{MW} \times 30$ min at KUR. After cooling among 5 to 10 days, the gamma-rays of medium and long half life radionuclides were measured. Also, a XRD was used to study chemical

structure of the 2 Chinese medicines of total 7 samples, which were produced in China and Japan.

RESULTS and DISCUSSION: All of *Niu Huang Jiedu Pian*, 3 samples produced in China, were contained from 2.2 to 8.6% of As and from 1.2 to 74 ppm of Hg. The main mineral was realgar by XRD, and the chemical structure of As was sulphide; As_4S_4 . We could not find the products except for Chinese one. On the other hand, among 4 samples, 2 of *Liushen Wan* were produced in China, and contained approx. 7% of As and 7.5% of Hg. Also, among 2 Japanese *Liushen Wan*, one for child was contained approx. 1% of As and 30ppm of Hg, and one for adult was contained approx. 550 ppm of As and 1.2 ppm of Hg. The main minerals of these 2 Chinese *Liushen Wan* were realgar and cinnabar by XRD; As_4S_4 and HgS. On the other hand, the main minerals of these 2 Japanese *Liushen Wan* were gold and calcite by XRD; Au and CaCO_3 . So, the same named medicines never contained same toxic elements with same level concentrations. Because the chemical structures were sulphide, they are not absorbed into a body, but just given a shock for the body. So, toxicity of the elements was no problems. Additionally, some minerals in Chinese medicines tended to contain other toxic elements like Co, Cr and Sb by INAA. Furthermore, almost all herbs contained low level concentration of Hg. It was considered the sources of Hg of low concentrations were not minerals but ground contamination or dust contamination in the air.

Conclusion: It was clarified that some Chinese medicine contained high concentration of toxic elements and many herbs contained low concentration of Hg; however, it was considered their chemical structures were not dangerous. At the same time, the safety images of Chinese medicines and herbs were not correct.

K. Mori, H. Yoshino, Y. Iinuma, T. Fukunaga, Y. Kawabata, S. Sato¹, H. Hiraka¹, K. Iwase², Y. Yamaguchi³, K. Enjuji⁴, K. Furuta⁴, and T. Kasai⁴

Research Reactor Institute, Kyoto University (KURRI)

¹High Energy Accelerator Research Organization (KEK)

²Department of Materials and Engineering, Ibaraki University

³Institute for Materials Research, Tohoku University

⁴Graduate School of Engineering, Kyoto University

INTRODUCTION: The B-3 beam port of Kyoto University Research Reactor (KUR) had long been used as a four-circle single-crystal neutron diffractometer (4CND). For the last decade, however, the 4CND was so old that its research activity on neutron science was quite low. Therefore, the 4CND needed to be replaced and a new neutron diffractometer has been required at the B-3 beam port. Also, the new neutron diffractometer (Compact multipurpose neutron diffractometer) is critical for the structural investigations of energy storage materials such as hydrogen absorbing alloys and rechargeable lithium-ion batteries. The neutron (powder) diffraction is a powerful tool to determine the positions of light elements (e.g., hydrogen and lithium) in solids. Here, we report the current status of the B-3 beam port of KUR and the preliminary neutron diffraction experiments using a hydrogen absorbing alloy.

INSTRUMENT: The compact multipurpose neutron diffractometer is now being installed on the B-3 beam port. The neutron wavelength (λ), which is monochromatized by the (220) plane of a Cu single crystal, is 1 Å. To cover the detector area ($6^\circ \leq 2\theta \leq 150^\circ$), 24 ³He tube detectors (1/2 inch in diameter) have been prepared. The distances from the monochromator to the sample and from the sample to the detector will be 1.9 m and 1.2 m, respectively. Fig. 1(a) shows the goniometer for the compact multipurpose neutron diffractometer; we performed an operation check. A detector bank including the 24 ³He tube detectors will be placed on an arm of the goniometer. In addition, the new beam shutter was installed at the B-3 beam port, as shown in Fig. 1(b).

PRELIMINARY EXPERIMENTS: The preliminary neutron diffraction experiments were performed using the hydrogen absorbing alloy, $(\text{Ti}_{0.31}\text{Cr}_{0.33}\text{V}_{0.36})\text{D}_{1.7}$, where D is the deuterium. It is worth noting that $\text{Ti}_{0.31}\text{Cr}_{0.33}\text{V}_{0.36}$ is a null alloy for neutron scattering due to its atomic compositions (i.e., $b_c[\text{Ti}_{0.31}\text{Cr}_{0.33}\text{V}_{0.36}] = 0$; $b_c[\text{Ti}] = -3.370$ fm, $b_c[\text{Cr}] = 3.635$ fm, and $b_c[\text{V}] = -0.443$ fm), where b_c is the coherent scattering length. The crystal structure has

been refined on the basis of a cubic CaF_2 -type structure with $a = 4.288(1)$ Å, using X-ray diffraction with Cu $K\alpha$ radiation (see Fig. 2(b)). As shown in Fig. 2(a), we succeeded to observe several Bragg reflections for the $(\text{Ti}_{0.31}\text{Cr}_{0.33}\text{V}_{0.36})\text{D}_{1.7}$ on the B-3 beam port; which could be indexed on the basis of $\lambda = 1$ Å. Note that the Bragg reflections correspond to the D-D correlations because of the null alloy.

Furthermore, the data acquisition group of the neutron science division of KEK (KEK-KENS DAQ group) has used the B-3 beam port to assess their new ⁶Li-glass neutron detector system, LiTA12. The LiTA12 system consists of a ⁶Li-glass neutron detector with a multianode photo multiplier tube (MA-PMT), an amplifier, and an analog-to-digital converter (ADC) board. The B-3 beam port has a wide space around the sample position; therefore we can easily install any other system like the LiTA12 system.

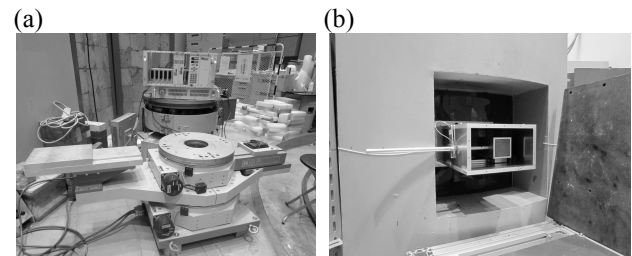


Fig. 1. Current status of the B-3 beam port of KUR: (a) new goniometer for the CMND and (b) new beam shutter installed at the B-3 beam port.

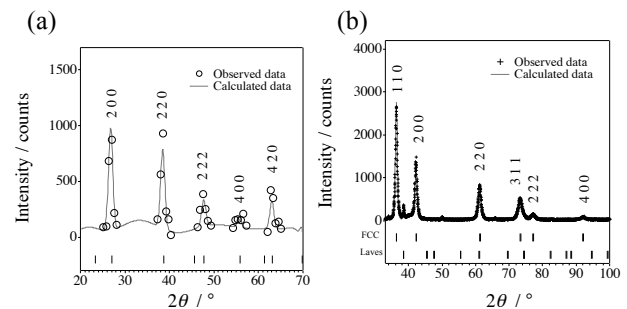


Fig. 2. Neutron and X-ray diffraction data for a hydrogen storage alloy, $(\text{Ti}_{0.31}\text{Cr}_{0.33}\text{V}_{0.36})\text{D}_{1.7}$, collected at (a) the B-3 beam port of KUR and (b) a X-ray diffractometer with Cu $K\alpha$ radiation.

採択課題番号 26007 材料研究および中性子検出器開発を目的とした
小型多目的中性子回折装置の建設

通常採択

(京大・原子炉) 森一広、吉野泰史、飯沼勇人、福永俊晴、川端祐司 (高エネ研) 佐藤節夫、平賀晴弘 (茨城大・工) 岩瀬謙二 (東北大・金研) 山口泰男 (京大院・工) 延壽寺啓吾、古田幸三、笠井拓矢

CO1-3 Synthesis of Metal Nanoparticles under the Gamma-ray Irradiation Field

F.Hori, T.Hori, A.Tohkai, H.Nakanishi, A.Iwase,
M.Sakamoto²

Dept. of Mater. Sci., Osaka Prefecture University
¹Research Reactor Institute, Kyoto University

INTRODUCTION: It is known that metallic nanoparticles have some specific properties, which are not appear in bulk materials such as catalytic activities, magnetic properties and so on. Also the character of them depends on its size, shape, structure, chemical composition and so on. For instance, it is known that Au nanoparticles exhibit the surface plasmon resonances (SPRs) in specific wavelength at about 520 nm. They have many possibilities to applied for various industrial fields. Generally, many kinds of metal nanoparticles commercially are synthesized by using chemical reaction method. On the other hands, it has been reported that specific feature of metallic nanoparticles can be synthesized under energetic irradiation fields, such as ultrasonic, electron, gamma-ray, plasma and so on. Using these irradiation reduction methods, it is possible to fabricate the unexpected structured nanoparticles. So far, we have successfully synthesized Cu nanoparticles, which is not easy to reduce in aqueous solution by chemical reaction, by using gamma-ray irradiation reduction method [1]. However, many of them are not only pure Cu but also copper oxides. In this study, we have tried to fabricate pure Cu nanoparticles by adding of ethylene glycol instead of diethylene glycol.

EXPERIMENTS: Aqueous solutions with a given concentration of copper complex $((\text{CH}_3\text{COO})_2\text{Cu}\cdot\text{H}_2\text{O})$ with an additive of sodium dodecyl sulfate (SDS) and ethylene glycol (EG). The solution was argon gas purged and sealed into polystyrene vessels. They were irradiated at about 300 K with 1.17 and 1.33 MeV gamma-rays from ^{60}Co radio active source at gamma irradiation facility in KURRI, Kyoto University. The total dose was fixed to 23.4 kGy with dose rate of 15.6 kGy/h. UV-vis absorption spectra were measured by using Shimadzu UV-2550 spectrophotometer in the wavelength range in 300-800 nm and the shapes and the structures for all colloidal products were observed by conventional TEM

(JEOL JEM-2000FX). Samples for TEM observations were made by putting a drop of colloidal solutions on a carbon film with a Mo mesh and dried them in a vacuum.

RESULTS:

Figure 1 shows the UV/vis absorption spectra for aqueous solutions before and after gamma-ray irradiation. It appears only one absorption peak around 570 nm, which shows pure Cu nanoparticles production, after gamma-ray irradiation. This is quite different from the result that of adding of DEG [1]. This result clearly shows that only pure Cu nanoparticles were generated and no oxidation takes place during gamma-ray irradiation. This is because ethylene glycol act as the scavenger of oxidation radicals from H_2O by gamma-ray irradiation radiolysis. TEM observation shows that generated particles are monodisperse spherical shape and its average diameter is about 17 nm (fig. 2).

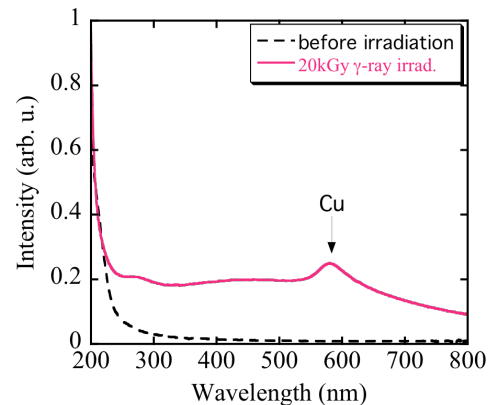


Fig. 1 UV/vis absorption spectra of aqueous solutions including Cu-ions before and after gamma-ray irradiation.

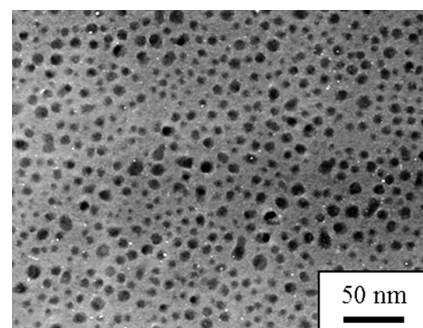


Fig. 2 TEM image of synthesized Cu nanoparticles by gamma-ray irradiation reduction.

References

- [1] T.Hori, K.Nagata, A.Iwase and F.Hori, Jpn. J. Appl. Phys. 53(5), 2014

CO1-4 The Role of Human Oxidation Resistance 1 (OXR1) in Cellular Response to Radiation

A. Matsui, Y. Yoshikawa, A. Yamasaki, T. Saito¹, N. Fujii¹, K. Tano¹, Q. Zhang-Akiyama

Graduate School of Science, Kyoto University
¹Research Reactor Institute, Kyoto University

INTRODUCTION: OXR1 (oxidation resistance 1) is a gene highly conserved in eukaryotes. Previous studies showed that human OXR1 suppressed spontaneous mutation in *E. coli mutH nth* [1]. OXR1 is induced by oxidative stresses such as H₂O₂ and is localized to mitochondria [2]. However, the function of OXR1 remains to be elucidated. Reactive oxygen species (ROS) act as a mediator of ionizing radiation -induced cellular damage. To clarify the protective functions of OXR1 against oxidative damage, we studied the effects of OXR1 on radiation -generated damage. In this study, we used gamma -ray and high LET heavy -ion beams, which are known of stronger cell killing effect than X -rays (3). Our studies showed that OXR1 proteins in HeLa cells were induced by carbon -ion beam, and that OXR1-knockdown HeLa cells were highly sensitive to heavy -ion beams. This year, we found higher micronucleus formation rate in the cells after irradiation. Then, the cells were released from cell cycle check point earlier than control cells. To study the function of OXR1 further, we are now under constructing OXR1-knockout DT40 cells.

EXPERIMENTS:

Irradiation

HeLa cells stably expressing shRNA targeting OXR1 or luciferase were synchronized at G1/S phase, and irradiated with gamma -ray (0.77 Gy/min), carbon -ion (290MeV/nucleon, 87.0keV/um) or iron -ion (500MeV/nucleon, 64.83 mmH₂O) beams generated by the Heavy Ion Medical Accelerator in Chiba (HIMAC). The irradiated cells were incubated for about 24 or 34 h, and fixed. The cells were used in the following experiments.

Micronucleus formation

The nuclei were counter -stained with DAPI. The micronuclei were detected with fluorescence microscopy.

Cell cycle analysis

Nuclei were stained with 50 ug/mL PI. The samples were analyzed with FACS.

Targeted disruption of OXR1 in DT40 cells

We prepared chicken OXR1 disruption constructs using puromycin, blasticidin or histidinol resistance gene. The chicken B lymphoma cells DT40 are cultured and transfected with the three gene disruption constructs.

RESULTS: The chicken OXR1 targeting constructs, OXR1-pur, OXR1-bsr and OXR1-his were generated. DT40 cells are now transfected with electroplation method. OXR1 -knockout DT40 cells are not gained.

FUTURE PERSPECTIVE: We will try constructing OXR1 -knockout TD40 cells. After finishing the step, we will study radation -induced ROS, DNA damages and cell death of the constructed cells.

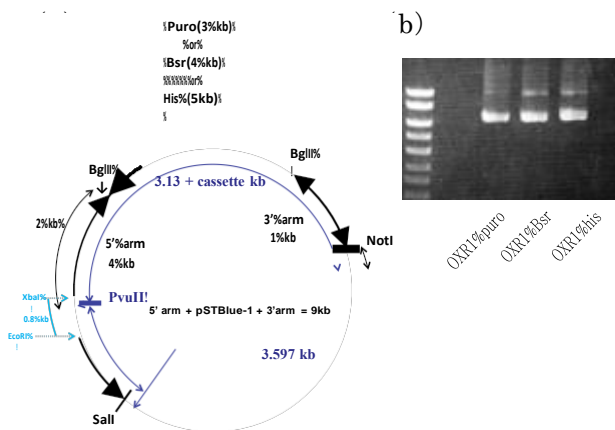


Fig. 1. (a) Schematic representation of the OXR1 disruption constructs. (b) Electrophoresis of three constructs.

REFERENCES:

- [1] M.R. Volkert *et al.*, Proc. Natl. Acad. Sci., (2000) **97**, 14530-14535.
- [2] N.A. Elliott, M.R. Volkert, Mol. Cell Biol., (2004) **24**, 3180-318.
- [3] M. Suzuki *et al.*, Int. J. Radiat. Oncol. Biol. Phys., (2000) **48**, 241-250

CO1-5 Development of an Advanced Optical Fiber Type Neutron Detector

K. Watanabe, Y. Kumagai, A. Uritani, A. Yamazaki, Y. Sakurai¹ and H. Tanaka¹

Graduate School of Engineering, Nagoya University
¹Research Reactor Institute, Kyoto University

INTRODUCTION: The Boron Neutron Capture Therapy (BNCT) has been developed as one of the promising radiotherapies. In this radiotherapy, the neutron dose evaluation is quite important. Therefore, we are developing a novel small neutron flux monitor using an optical fiber. A small size optical fiber type neutron detector is one of the promising candidates of the on-line small neutron flux monitors in BNCT. The conventional optical fiber neutron detectors, however, show no peak shape corresponding to the neutron absorption reactions, in a pulse height spectrum due to the non-uniform and/or poor light collection [1-3]. These conventional detectors used ZnS-LiF, Li glass or plastic scintillators. On the other hand, we apply a new neutron scintillator Eu:LiCaAlF₆. This scintillator has some excellent properties, such as high light yield, high lithium content, transparency and chemical stability. The light yield of this scintillator is approximately 5 times higher than that of the Li glass.

Figure 1 shows the conceptual drawing of the small size optical fiber type neutron detector. Features of our detector are use of a bright scintillator and a quite small scintillator size. The scintillator size is controlled larger than ranges of ⁶Li(n,t) reaction products and smaller than ranges of fast electrons induced by gamma rays to suppress the signal pulse height only for gamma-ray induced events.

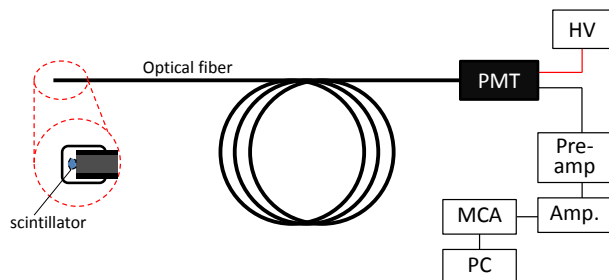


Fig. 1 Conceptual drawing of the optical fiber type neutron detector.

So far, we evaluated dynamic range and long term stability of our detector. Our detector was confirmed to show good linearity up to 10⁹ n/cm²/s. However, peak pulse height decreases due to neutron irradiation. In this report, we experimentally evaluate neutron radiation hardness of the developed detector.

RADIATION HARDNESS TEST: We fabricated the optical fiber type neutron detector using a small Eu:LiCaAlF₆ scintillator and experimentally evaluated its radiation hardness at the Heavy Water Neutron Irradiation Facility (HWNIF) of Kyoto University Research

Reactor (KUR). One of the reasons of decrease of the peak pulse height is expected to be reduction of the transmittance of the optical fiber. We, therefore, irradiated neutrons to the optical fiber used in our detector. The neutron flux was 10⁹ n/cm²/s. We continuously measured the transmittance of the optical fiber by using a spectrometer during the neutron irradiation. The transmittance of the fiber $T(t)$ decreases as;

$$T(t) = T_0 \exp(-t/\tau)$$

where T_0 ; initial transmittance, τ , life time of the optical fiber. We can determine the lifetime by fitting this equation to the experimental data of decrease of the optical fiber transmittance. Figure 2 shows the wavelength dependence of the lifetime of the optical fiber under neutron irradiation with 10⁹ n/cm²/s. The lifetime in infrared region is confirmed to be longer than that in ultraviolet and visible region. The emission wavelength of the Eu:LiCaAlF₆ scintillator is 380 nm, where the lifetime of the transmittance is not so long. From these results, one of the reasons of decrease of the peak pulse height is confirmed to be reduction of the transmittance of the optical fiber.

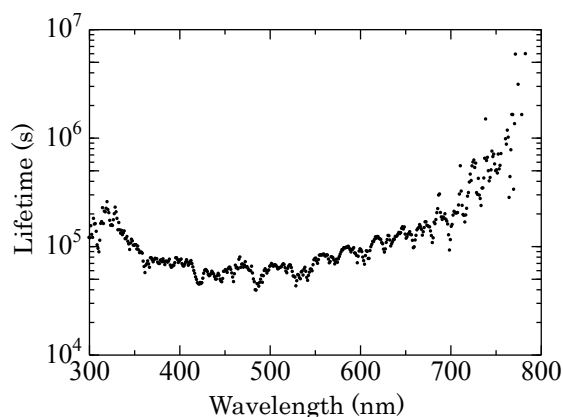


Fig. 2 Wavelength dependence of the lifetime under neutron irradiation.

In infrared region, the neutron radiation hardness is quite high. If we can use a neutron scintillator with infrared emission, the radiation hardness of the optical fiber type neutron detector can be improved.

REFERENCES:

- [1] M. Ishikawa *et al.*, Appl. Rad. Isotopes, **61** (2004) 775-779.
- [2] M. Ishikawa *et al.*, Nucl. Instr. Meth. A, **551** (2005) 448-457.
- [3] Y. Ito *et al.*, Radiat. Prot. Dosim., **110** (2004) 619-622.

CO1-6 Focusing Test of an Ellipsoidal Neutron Mirror with a Metal Substrate

M. Hino¹, J. Guo², S. Takeda³, T. Oda¹, S. Morita^{2*},
J. Kato², Y. Yamagata², M. Furusaka³, Y. Kawabata¹

¹Research Reactor Institute, Kyoto Univ., Japan

²RAP, RIKEN, Japan,

³Grad. Sch. of Eng., Hokkaido Univ., Japan

*Present address: Tokyo Denki Univ. Japan

INTRODUCTION: Progress of neutron optical devices is significant, however, it is still very difficult for neutron aspherical focusing mirror. Because the required surface roughness is smaller than 0.5 nm even for $m=3$ supermirror coating and the mirror size is large. In order to realize large ellipsoid neutron focusing mirror, we are doing several trials. In this study, we show the neutron focusing experimental result of ellipsoid mirror with a metal substrate. In general it is very difficult to make a smooth surface on metal due to the grain structure. By using electroless nickel-phosphorus (NiP) plated material, we can overcome this problem. Electroless NiP has great advantages for realizing neutron mirror because of its amorphous structure, good machinability and relatively large critical angle of total reflection for

neutrons without supermirror coating.

EXPERIMENTS: The design, manufacturing and polishing of the mirror were carried out by RIKEN [1]. The form accuracy of the mirror was estimated to be 5.3 μm Peak-to-Valley (P-V) and 0.8 μm P-V for the minor-axis and major-axis direction respectively, while the surface roughness was reduced to 0.2 nm rms. The neutron focusing performance of the mirror was evaluated using CN3 beam line at Kyoto University Research Reactor (KUR-CN3).

RESULTS: As shown in Fig.1, the two-dimensional (2D) image of neutron beam reflected by an ellipsoid focusing mirror was clearly changed as a function of distance between the mirror center and detector. Cadmium (Cd) pinhole with an aperture size of 1 mm in diameter to choose incident beams from the CN3 guide a Cd U-shape slit to remove unnecessary neutron beams affecting the focusing. The circular focusing spot at the focal point was almost equivalent to that of the pinhole.

REFERENCES:

[1] J.Guo, et al., Optics Express, 22(2014)24666-24677.

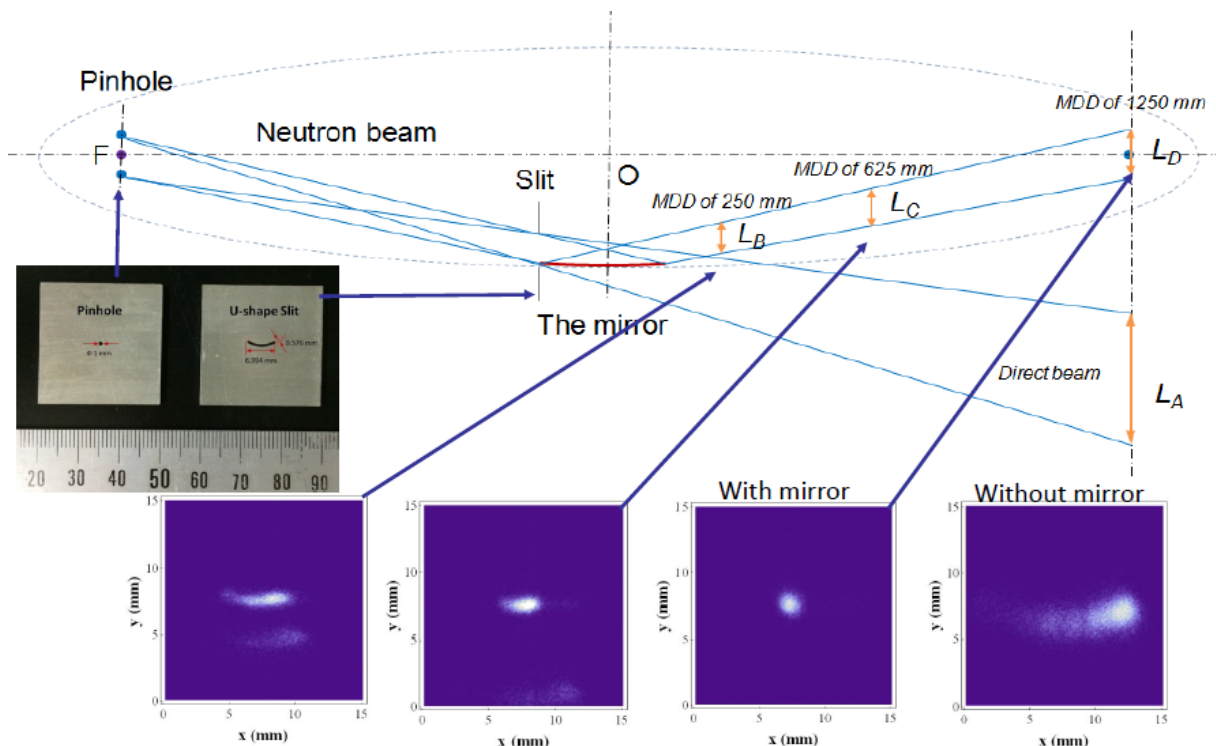


Fig.1 Schematic layout of neutron focusing experiment at KUR-CN3 and the 2D images of beam shapes as a function of the mirror center to detector distance (MDD), and the direct beam shape without the focusing mirror at the focal point.

採択課題番号 26065 次期中性子ビーム科学施設のための中性子光学デバイス開発 通常採択
(京大・原子炉) 日野正裕、小田達郎、川端祐司 (KEK・IMSS) 山田悟史、遠藤仁、瀬戸秀紀
(理研) 郭江、森田晋也、加藤純一、山形豊 (北大) 武田晋

CO1-7 Examination of the Usefulness as the New Boron Compound of KA-BSH for Born Neutron Capture Therapy

Gen Futamura¹, Shinji Kawabata¹,
Shin-Ichi Miyatake², Toshihiko Kuroiwa¹,
Yoshihide Hattori⁴, Mitsunori Kirihata⁴, Hiroki Tanaka³,
Yoshinori Sakurai³, Shin-Ichiro Masunaga³, Koji Ono³

¹Department of Neurosurgery, Osaka Medical College

²Division for Advanced Medical Development, Cancer Center, Osaka Medical College

³Research Reactor Institute, Kyoto University

⁴Osaka Prefecture University

INTRODUCTION:

Boron neutron capture therapy (BNCT) is an attractive technique for malignant brain tumor treatment. [1] It is important to have a significant differential uptake of ¹⁰B between tumor cells and normal cells to achieve potent tumor-selective antitumor effects. Today, clinically used dodecaboranethiol (BSH) is transferred to brain tumors only through the disrupted blood-brain barrier (BBB), so it is difficult for BSH to reach regions that tumor cells invade microscopically where the BBB seems to be normal. On the other hand, boronophenylalanine (BPA), which transfers boron via L-type amino acid transporter, can deliver ¹⁰B even in the infiltrating tumor cell population where the BBB is normal. However, some amounts of ¹⁰B are inevitably taken into the normal cells by BPA systemic administration. A wide variety of boron delivery agents have been synthesized to solve these problems. [1] Kojic acid (KA) was reported as the agent which showed intense uptake in malignant tumor. Therefore, we designed and synthesized KA-BSH and evaluated therapeutic effect of KA-BSH as boron delivery agents for BNCT in F98 glioma cell bearing rat brain tumor model.

MATERIALS AND METHODS:

BNCT was performed 14 days following stereotactic implantation of 10³ F98 glioma cells implanted rat brain tumor model. Rats were transported to the Nuclear Reactor Laboratory at Kyoto University Research Reactor Institute.

Based on the results of the biodistribution study, we prepared 4 groups. The rats were then randomized on the basis of weight into experimental groups of 6-8 animals each as follows: Group 1, KA-BSH administered by in-

travenous administration (iv) and neutron irradiated; Group 2, KA-BSH administered by convection enhanced delivery (CED) by using Alzet pump, which can deliver solutions directly into the solid tissue with continuous pressure gradient distribution [2, 3], and neutron irradiated; Group 3, neutron irradiation; Group 4, untreated controls. BNCT was initiated 1 h after termination of Alzet pump infusion or i.v. administration. All irradiated rats were anesthetized with a pentobarbital sodium. The rats were irradiated for 60 min with 1MW. The antitumor effects of BNCT were evaluated in the mean survival times (MSTs) of the rat.

RESULTS:

The estimated physical radiation doses delivered to tumor, brain and blood were calculated according to boron concentrations. The physical radiation doses delivered to the tumor were 1.1Gy for KA-BSH administered by iv. The corresponding normal brain doses were 1.0Gy. The survival data of Group 1, 2, 3 and 4 following BNCT showed that the MSTs were 35.4±8.0 days, 29.8±3.3 days, 30.2±2.2 days and 28.5±3.1 days, respectively. We accepted significantly extend the duration of survival time of the rats group using KA-BSH administered by iv (Group 1), compared with the neutron irradiation only (Group 3) (p<0.005).

CONCLUSION:

Survival times of group1 were significantly prolonged even compared with irradiation group. The therapeutic effect of KA-BSH administered by iv was higher than that we expected from these tissue boron concentrations and physical radiation doses. This study suggested that KA-BSH might have extremely high compound biological effectiveness (CBE), and KA-BSH might be the drug to add therapeutic effect of clinical BNCT using BPA or in combination with BPA / BSH to.

REFERENCES:

- [1] Barth RF *et al*: Radiat Oncol 7: 146, 2012.
- [2] Hiramatsu R *et al*: J Pharm Sci 104: 962-70, 2015
- [3] Kawabata S *et al*: J Neurooncol 103: 175-85, 2011